



Figures and figure supplements

Molecular basis of wax-based color change and UV reflection in dragonflies

Ryo Futahashi et al

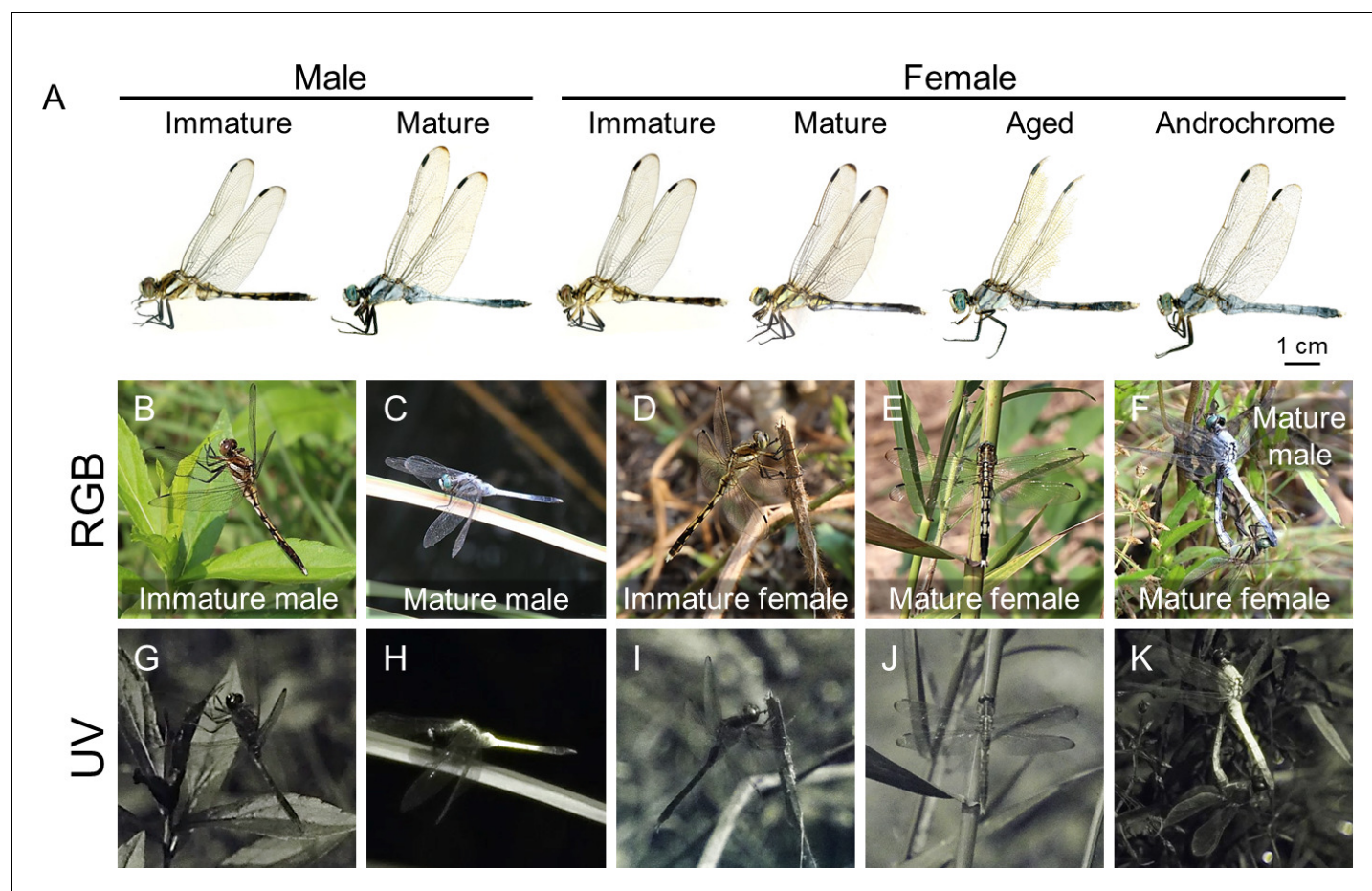


Figure 1. Stage- and sex-dependent adult color change in *O. albistylum* as visualized in red, green, blue (RGB) and ultraviolet (UV) light. (A) Adult males and females of *O. albistylum*. (B, G) Immature male. (C, H) Mature male. (D, I) Immature female. (E, J) Mature female. (F, K) Mating pair. Images photographed normally (B–F) or through a UV filter (G–K) in the field.

DOI: <https://doi.org/10.7554/eLife.43045.003>

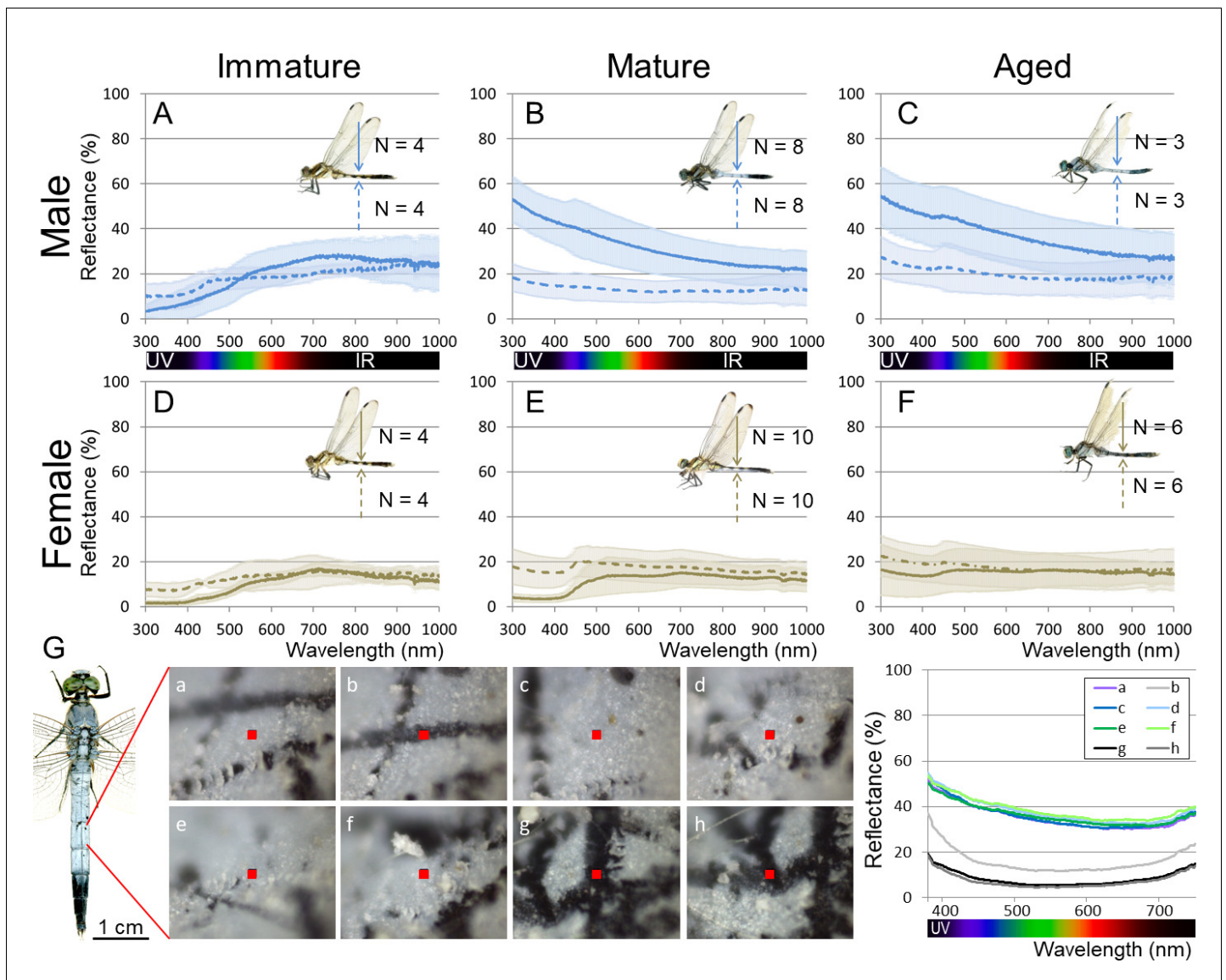


Figure 2. Reflectance of the adult body surface at the 5th abdominal segment of *O. albistylum*. (A–F) Spectrometry of a round area (6 mm in diameter) in males (A–C) and females (D–F). (A, D) Immature individuals. (B, E) Mature individuals. (C, F) Aged individuals. Solid and dotted lines indicate averaged UV reflectance on the dorsal and ventral sides of the abdomen, respectively. The standard deviation is shaded. (G) Micro-spectrometry of the 5th abdominal segment of a mature male. UV reflectance was measured in eight micro-areas (10 μ m \times 10 μ m each) depicted as red squares in the photos. In the photos, white areas are covered with secreted wax whereas black areas are without wax, presumably because of accidental scratches and cracks on the adult body surface.

DOI: <https://doi.org/10.7554/eLife.43045.004>

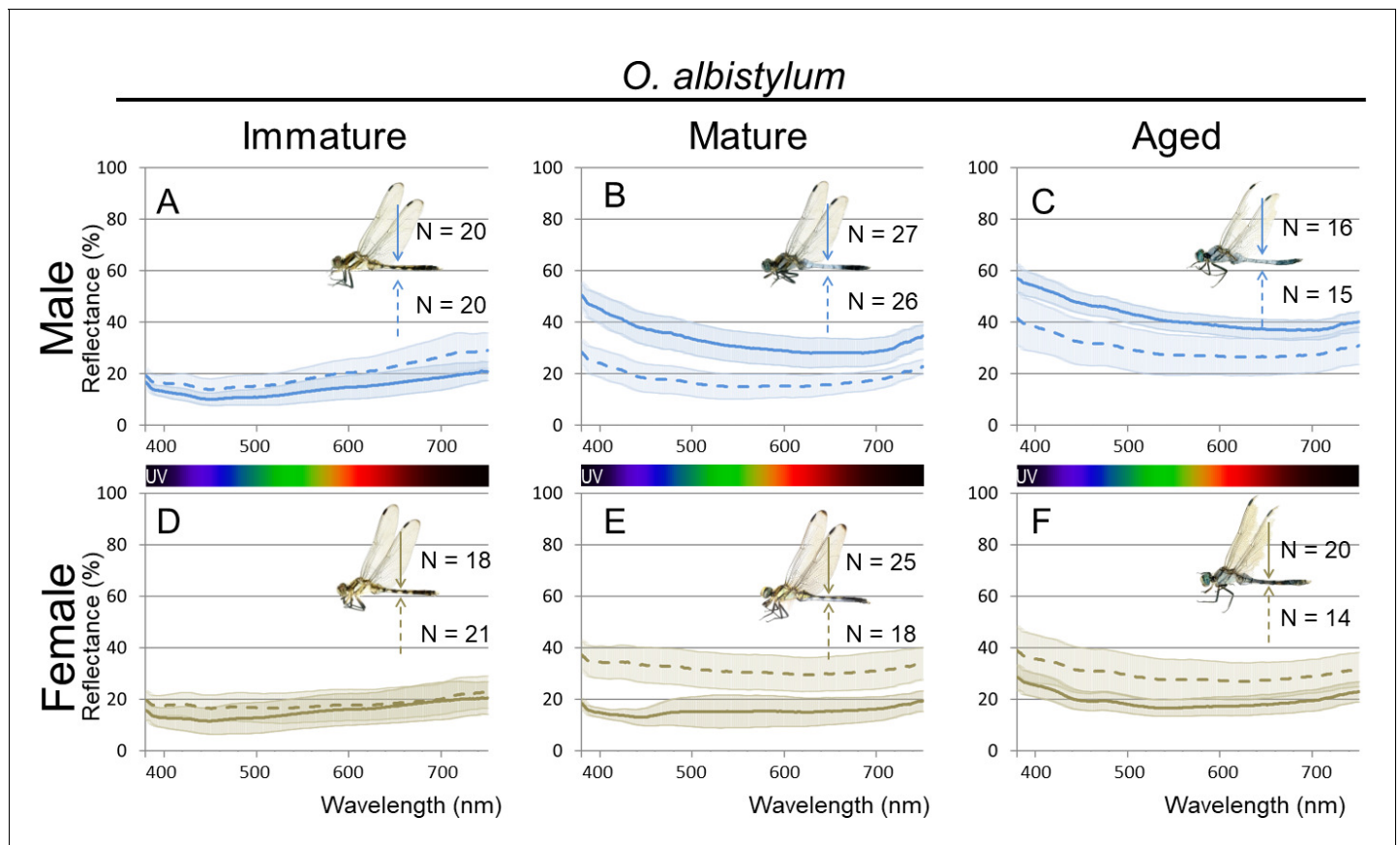


Figure 2—figure supplement 1. Micro-spectrometry (of $10 \times 10 \mu\text{m}$ micro-areas) of *O. albistylum*. (A–C) Male. (D–F) Female. (A, D) Immature individuals. (B, E) Mature individuals. (C, F) Aged individuals. Three to eight micro-areas were measured for each individual.

DOI: <https://doi.org/10.7554/eLife.43045.005>

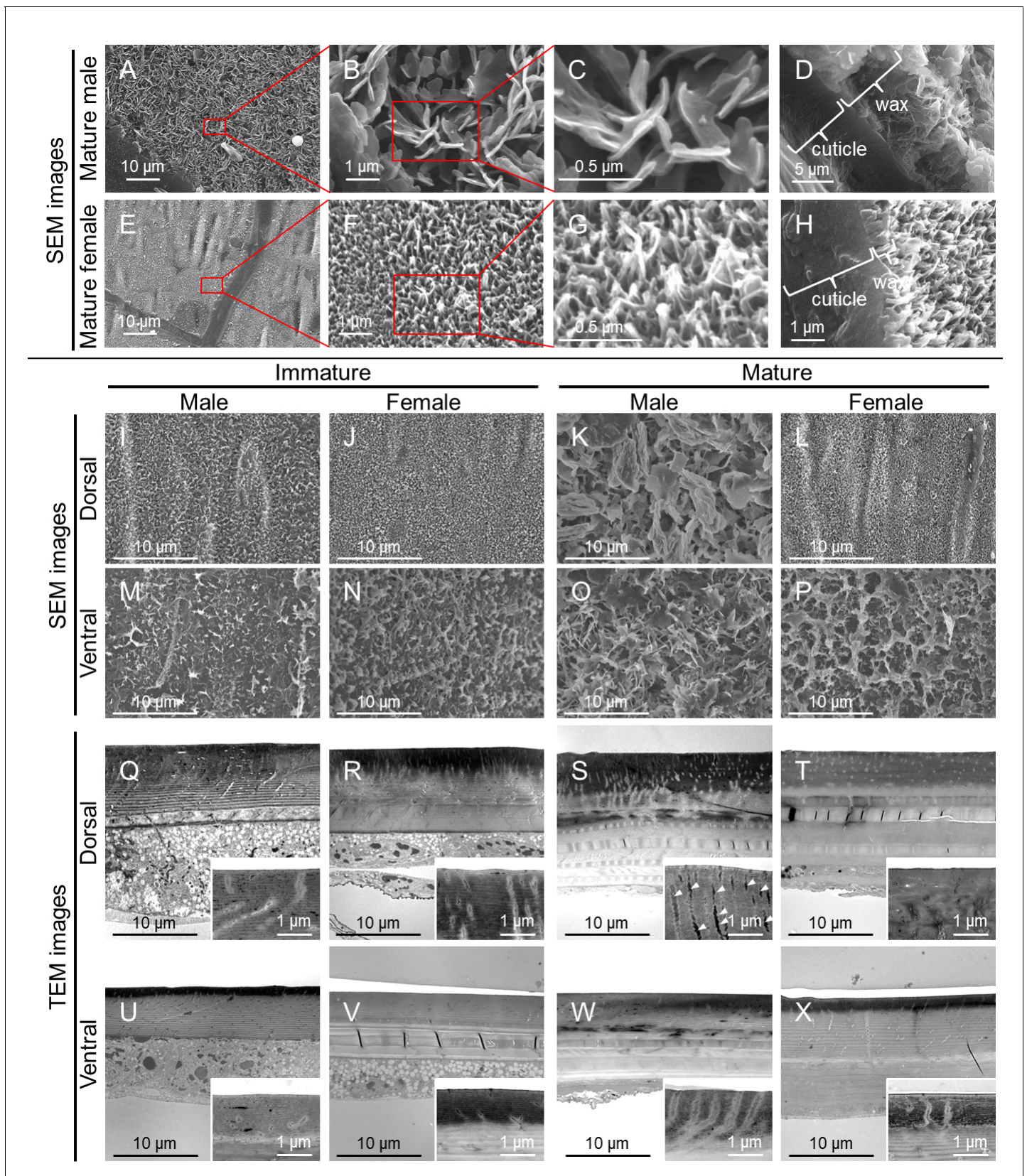


Figure 3. Fine structure of the adult body surface at the 5th abdominal segment of *O. albistylum*. (A–P) Scanning electron microscopic (SEM) images of the body surface. (Q–X) Transmission electron microscopic (TEM) images of the sectioned cuticle. It should be noted here that the surface wax was

Figure 3 continued on next page

Figure 3 continued

dissolved and removed during the processing of the sample for TEM observation. (A–H) Dorsal side of mature male (A–D) and mature female (E–H). Panels B and F are magnified images of panels A and E, as indicated by red rectangles. Likewise, panels C and G are magnified images of panels B and F. (D, H) Cross-sectioned images of cuticle and surface wax. (I–L and Q–T) Dorsal side. (M–P and U–X) Ventral side. (I, M, Q, U) Immature male. (J, N, R, V) Immature female. (K, O, S, W) Mature male. (L, P, T, X) Mature female.

DOI: <https://doi.org/10.7554/eLife.43045.014>

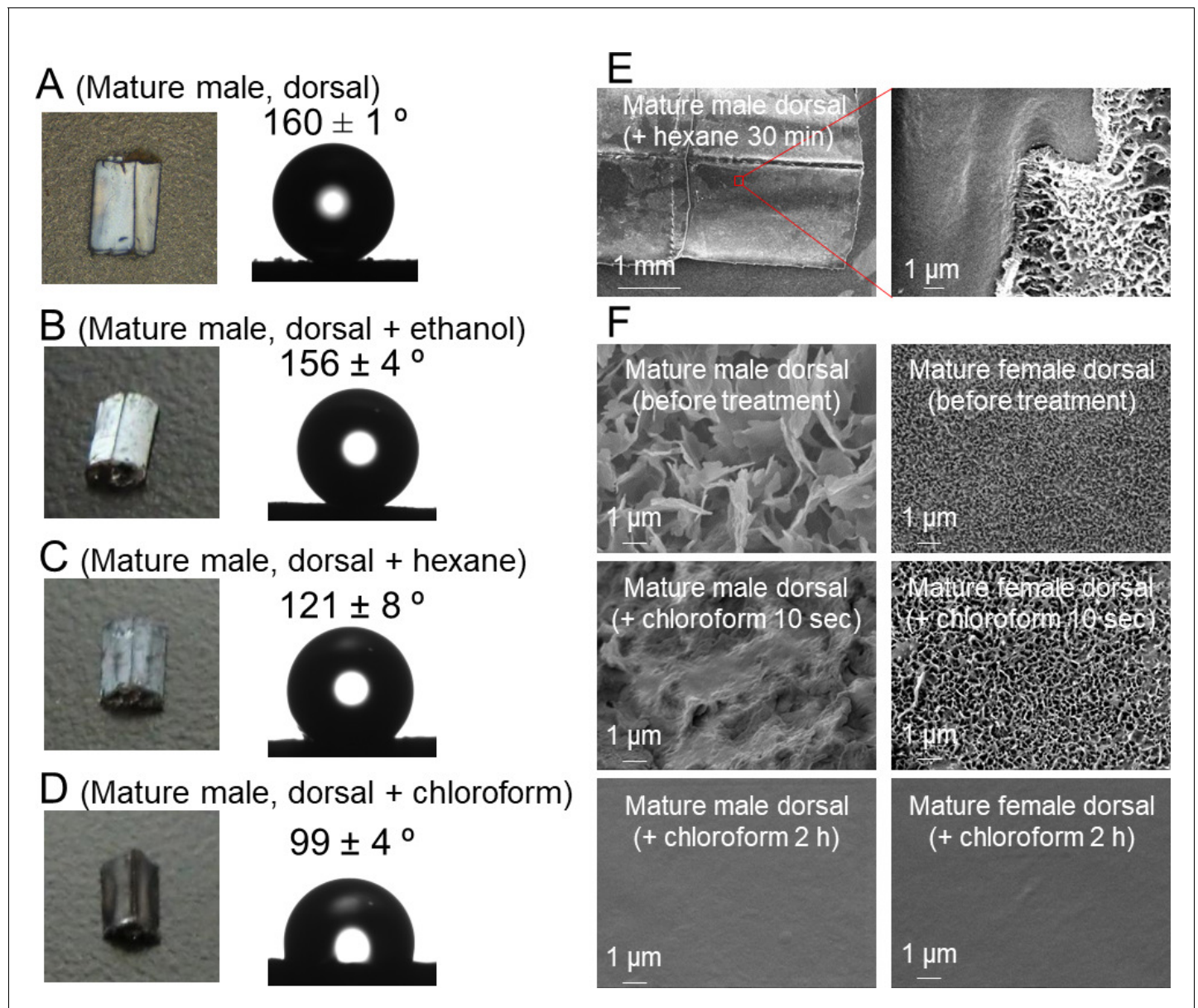


Figure 4. Solubility and wettability of the abdominal wax of *O. albistylum*. (A–D) Dorsal side of the 5th abdominal segment of mature males. (A) No treatment. (B) After ethanol treatment. (C) After hexane treatment. (D) After chloroform treatment. (E) Scanning electron microscope images of the dorsal surface of mature male 30 min after hexane treatment. (F) Scanning electron microscope images of dorsal side of a mature male (left) or a mature female (right) after chloroform treatment.

DOI: <https://doi.org/10.7554/eLife.43045.016>

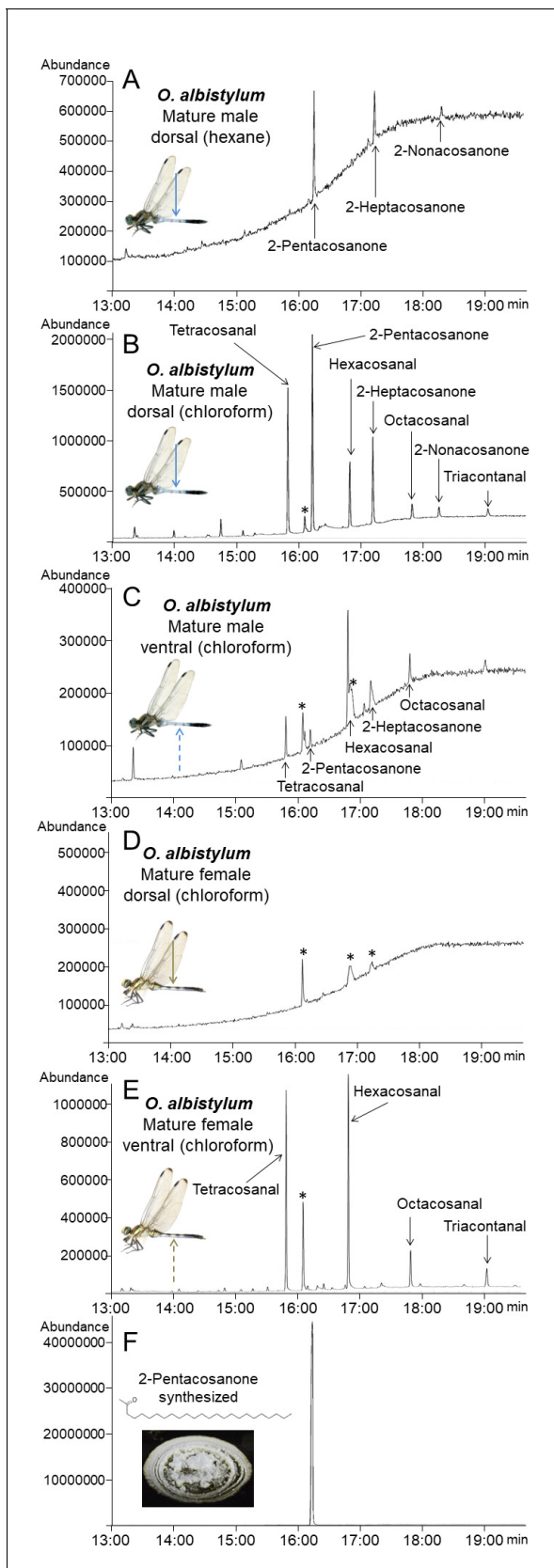


Figure 5. Identification and chemical synthesis of surface wax of *O. albistylum*. (A) Chromatogram of hexane extract from the dorsal abdomen of a mature male. (B) Chromatogram of chloroform extract from the dorsal abdomen of a mature male. (C) Chromatogram of chloroform extract from the ventral abdomen of a mature male. (D) Chromatogram of chloroform extract from the dorsal abdomen of a mature female. (E) Chromatogram of chloroform extract from the ventral abdomen of a mature female. (F) Chromatogram of synthesized 2-pentacosanone. *Figure 5 continued on next page*

Figure 5 continued

ventral abdomen of a mature male. (D) Chromatogram of chloroform extract from the dorsal abdomen of a mature female. (E) Chromatogram of chloroform extract from the ventral abdomen of a mature female. (F) Chromatogram of chemically synthesized 2-pentacosanone. Asterisks indicate nonspecific peaks that are also detected with the solvent only. The Y-axis shows the abundance of total ion current.

DOI: <https://doi.org/10.7554/eLife.43045.017>

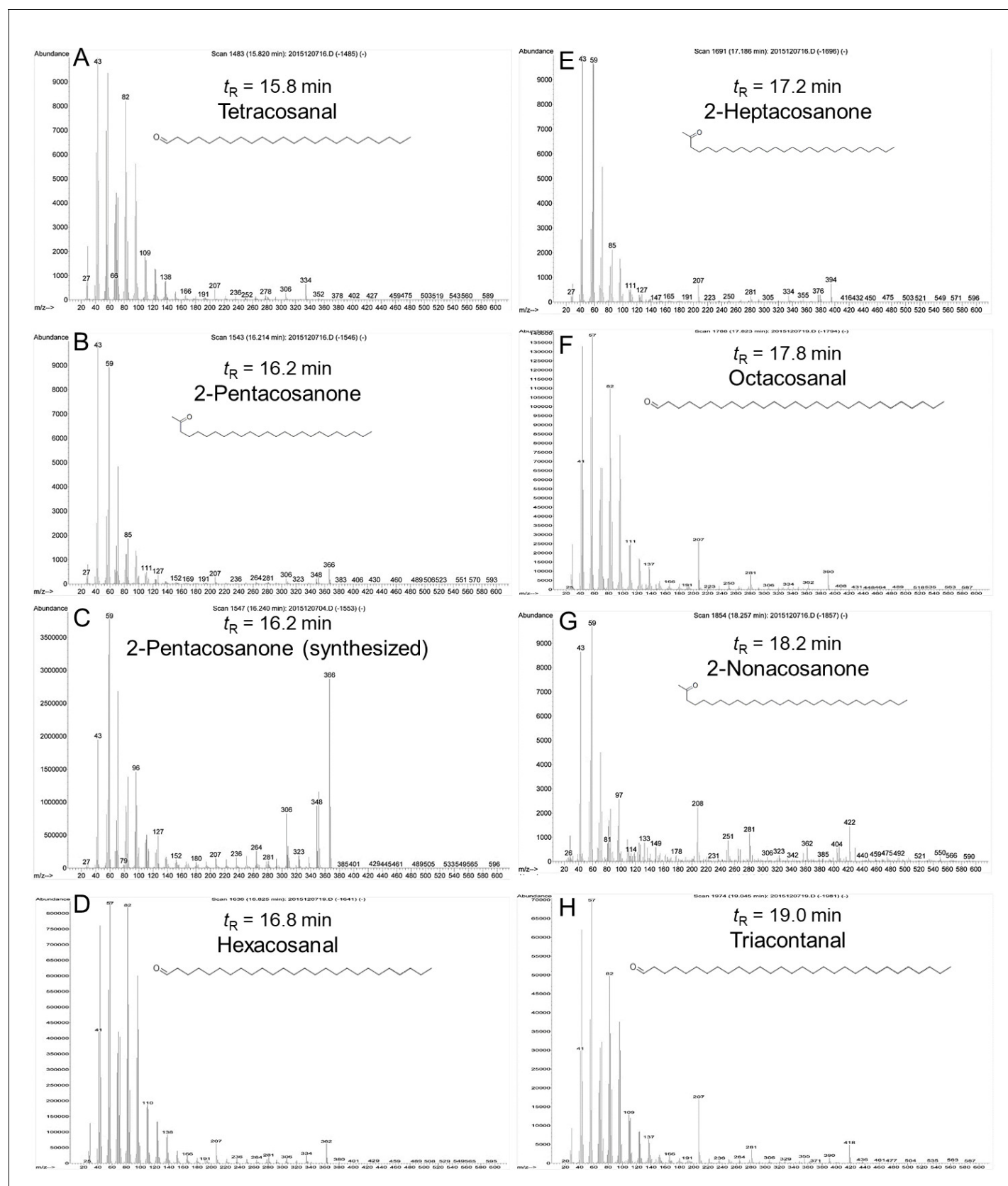


Figure 5—figure supplement 1. Mass spectra and extracted ion chromatogram of dragonfly wax (A, B, D–H) and of synthetic 2-pentacosanone (C).

DOI: <https://doi.org/10.7554/eLife.43045.018>

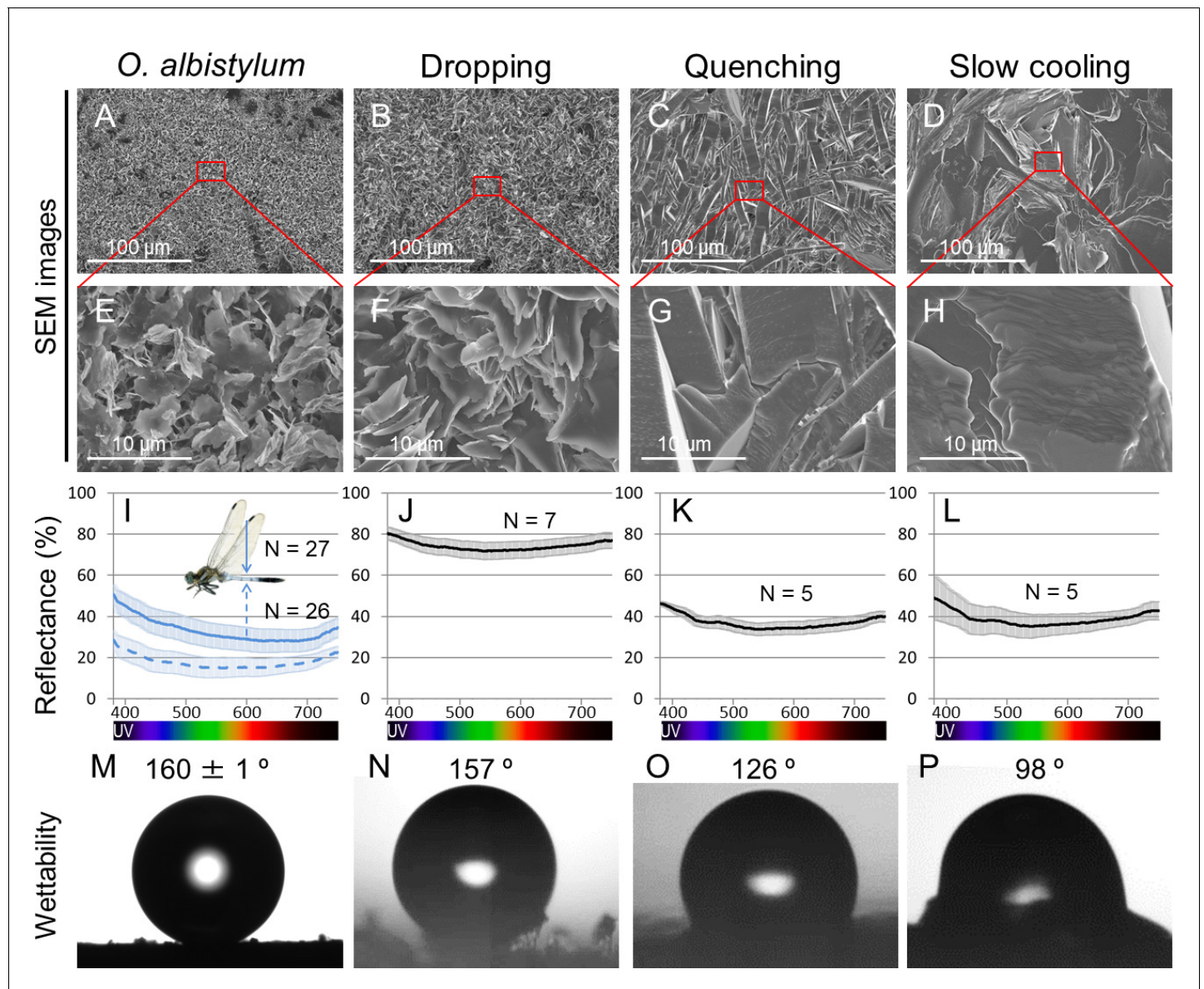


Figure 6. Comparison of surface fine structure, reflectance, and wettability between the dorsal abdomen of mature males of *O. albistylum* and synthetic 2-pentacosanone crystallized on glass plates using three different cooling processes. (A–H) Scanning electron microscope images. Panels E, F, G and H are magnified images of panels A, B, C and D, respectively, as indicated by red rectangles. (I–L) Micro-spectrometry from a $10 \mu\text{m} \times 10 \mu\text{m}$ area. (M–P) Wettability measured with a 1 nL water droplet. (A, E, I, M) The dorsal abdomen of mature males of *O. albistylum*. (B, F, J, N) Synthetic wax crystallized by the dropping method. (C, G, K, O) Synthetic wax crystallized by the quenching method. (D, H, L, P) Synthetic wax crystallized by the slow-cooling method.

DOI: <https://doi.org/10.7554/eLife.43045.019>

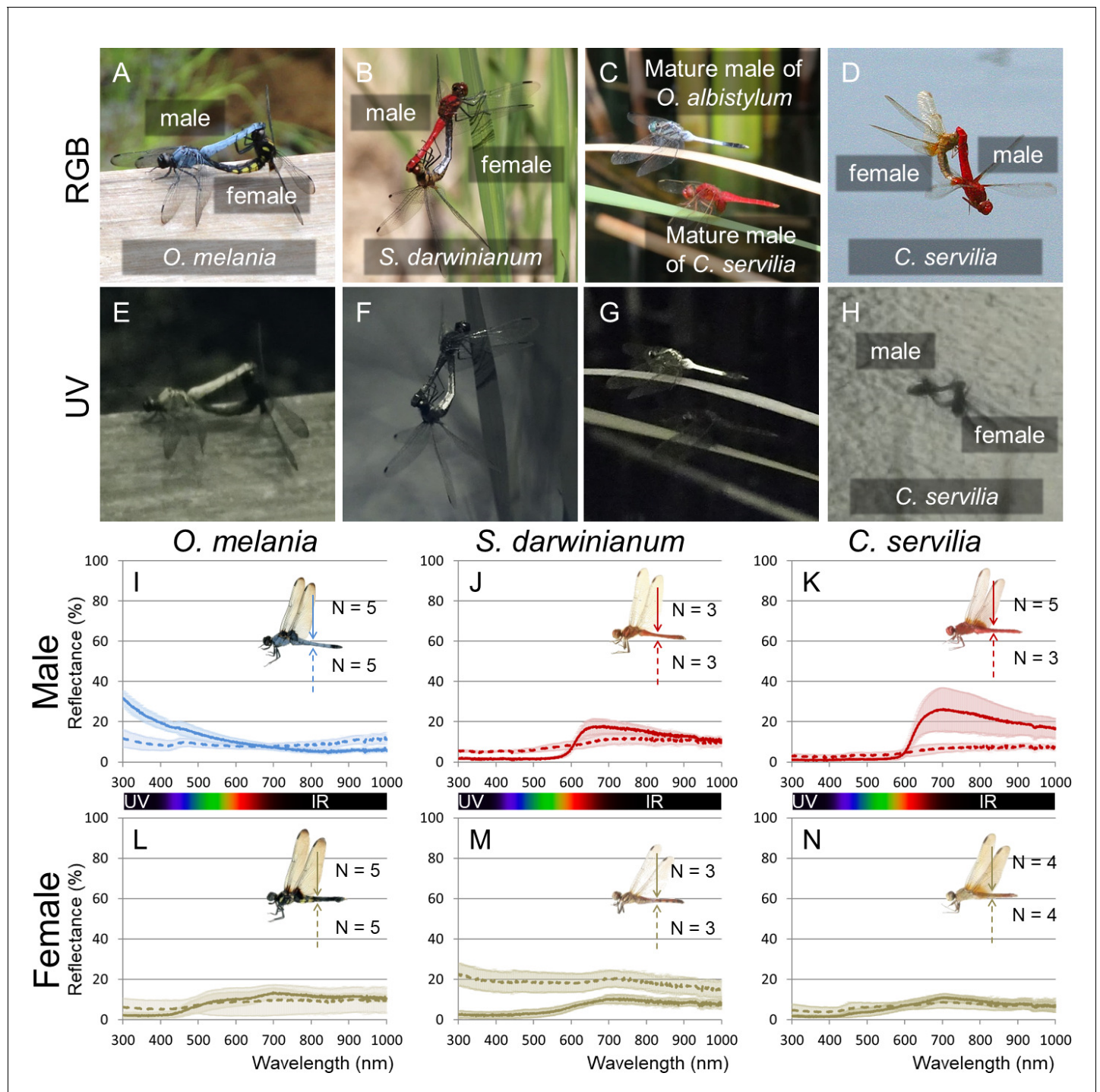


Figure 7. UV reflection patterns in *O. melania*, *S. darwinianum* and *C. servilia*. (A, E) Mating pair of *O. melania*. (B, F) Mating pair of *S. darwinianum*. (C, G) Mature male of *C. servilia* with mature male of *O. albistylum*. (D, H) Mating pair of *C. servilia*. Each image photographed normally (RGB) (A–D) or through a UV filter (E–H) in the field. (I–N) Spectrometry of a round area (6 mm in diameter) on the 5th abdominal segment of *O. melania* (I, L), *S. darwinianum* (J, M), and *C. servilia* (K, N). (I–K) Male. (L–N) Female. Solid and dotted lines indicate averaged UV reflectance on the dorsal and ventral sides of the abdomen, respectively. The standard deviation is shaded.

DOI: <https://doi.org/10.7554/eLife.43045.021>

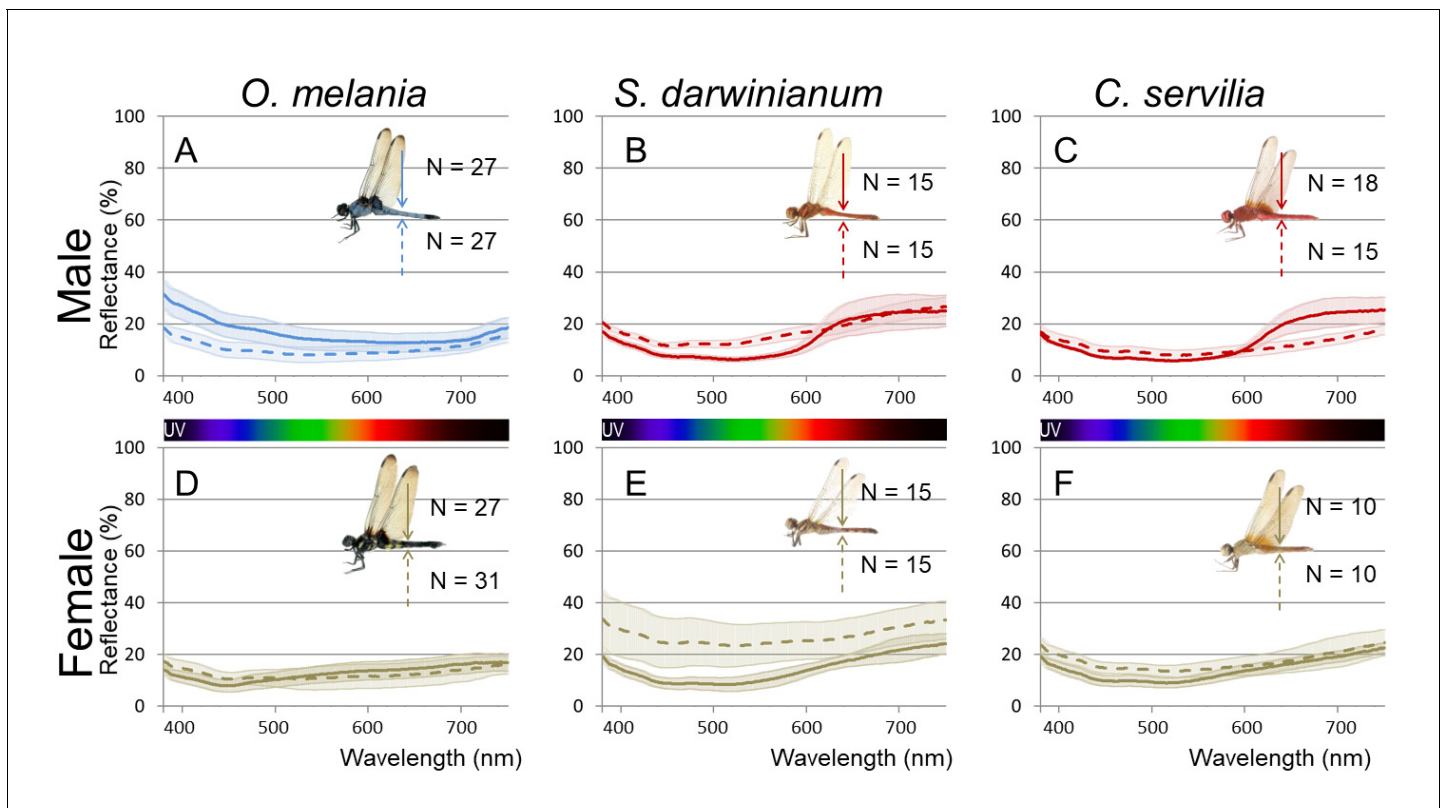


Figure 7—figure supplement 1. Micro-spectrometry (of a 10 × 10 μm micro-area) of *O. melania* (A, D), *S. darwinianum* (B, E), and *C. servilia* (C, F). (A–C) Male. (D–F) Female. Five to ten micro-areas were measured for each individual.

DOI: <https://doi.org/10.7554/eLife.43045.022>

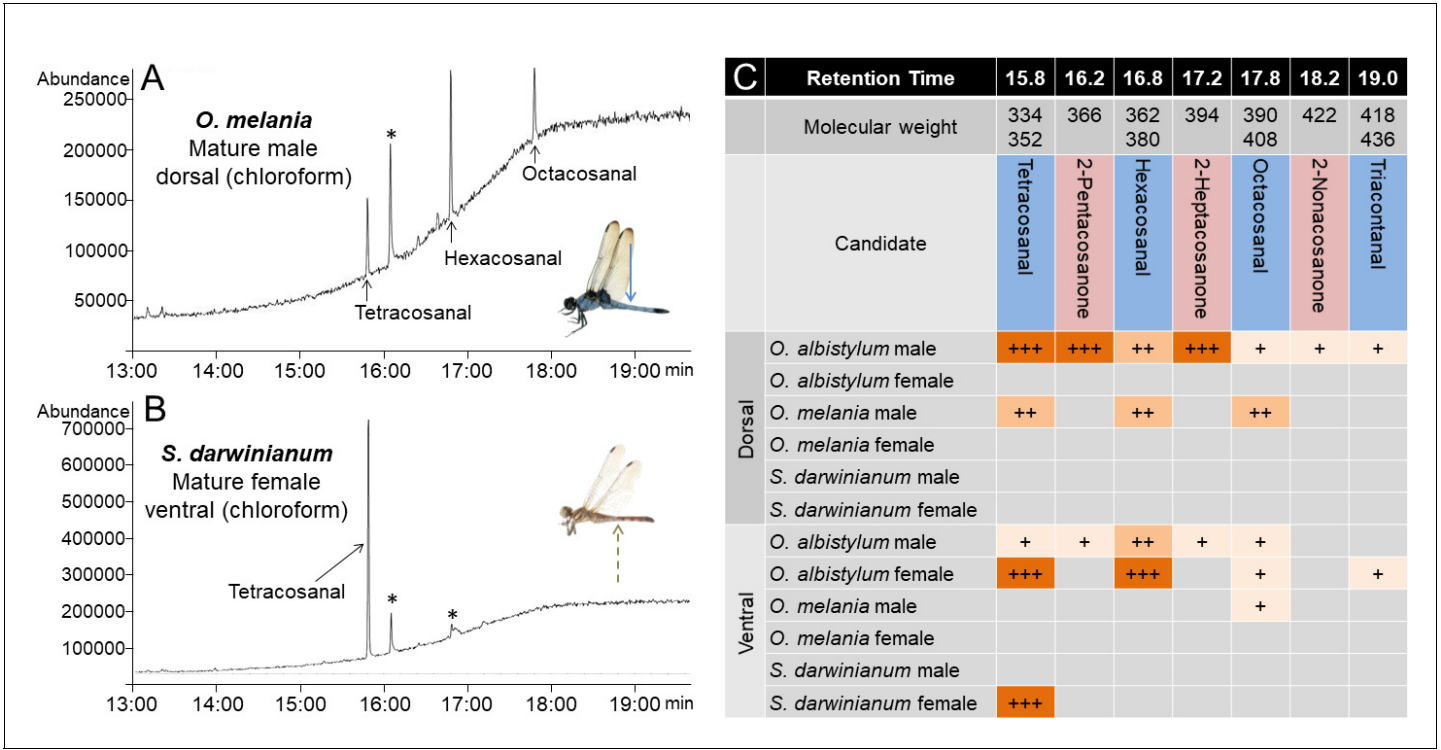


Figure 8. Comparison of wax components on the dorsal and ventral abdomen of *O. albistylum*, *O. melania* and *S. darwinianum*. (A) Chromatogram of chloroform extract from the dorsal abdomen of a mature male of *O. melania*. (B) Chromatogram of chloroform extract from the ventral abdomen of a mature female of *S. darwinianum*. Asterisks indicate nonspecific peaks also detected with the solvent only. (C) Summary of wax components detected from *O. albistylum*, *O. melania* and *S. darwinianum*. Relative amount was judged from the abundance of total ion current. +++, high amount; ++, moderate amount; +, small amount.

DOI: <https://doi.org/10.7554/eLife.43045.029>

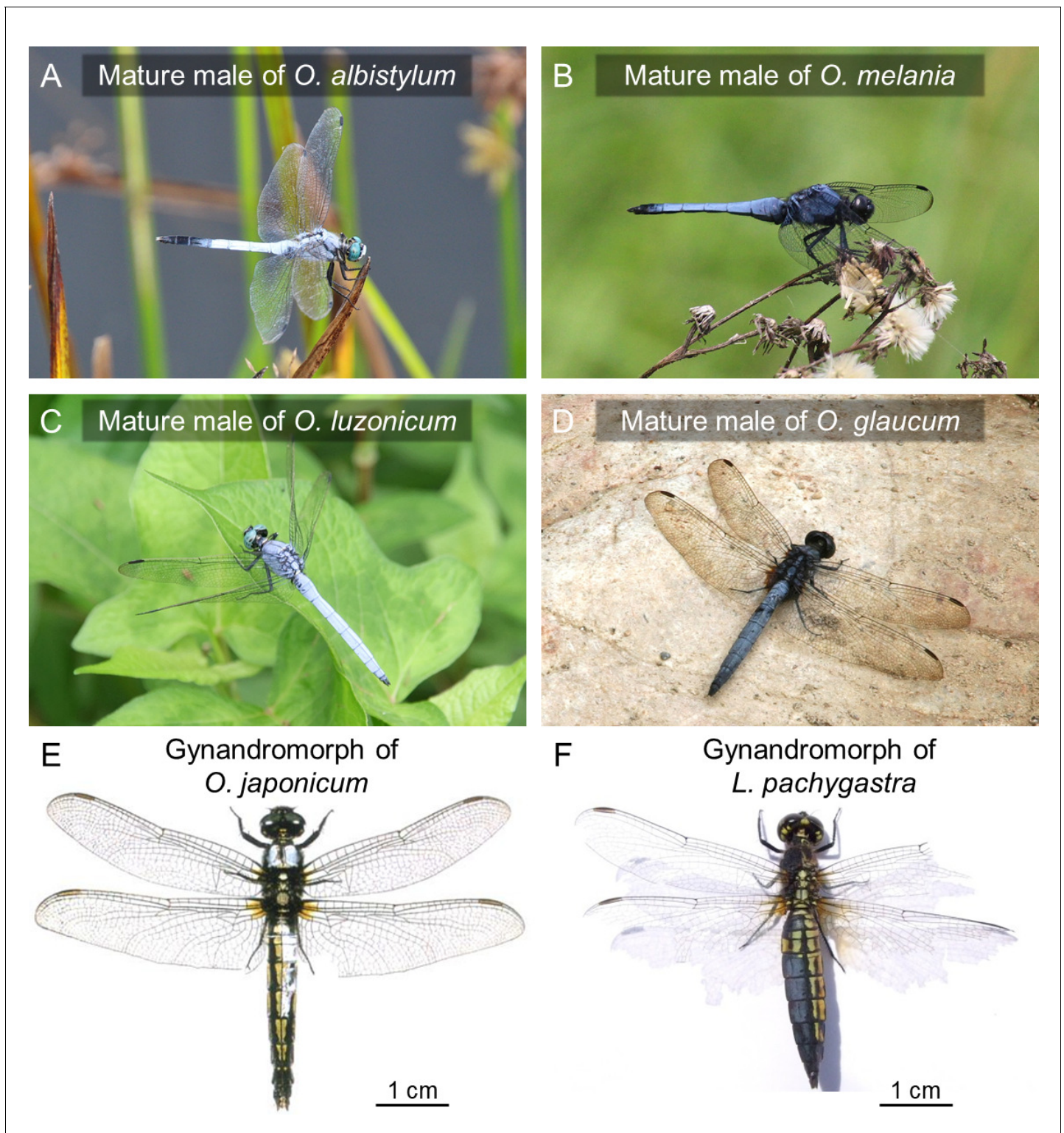


Figure 9. Surface wax of *Orthetrum* species and allied dragonflies. (A–D) Mature males of *O. albistylum* (A), *O. melania* (B), *O. luzonicum* (C) and *O. glaucum* (D). (E–F) Gynandromorphic individuals of *O. japonicum* (E) and *Lyriothemis pachygastra* (F). Photos courtesy of Mitsutoshi Sugimura (E) and Makoto Machida (F).

DOI: <https://doi.org/10.7554/eLife.43045.031>

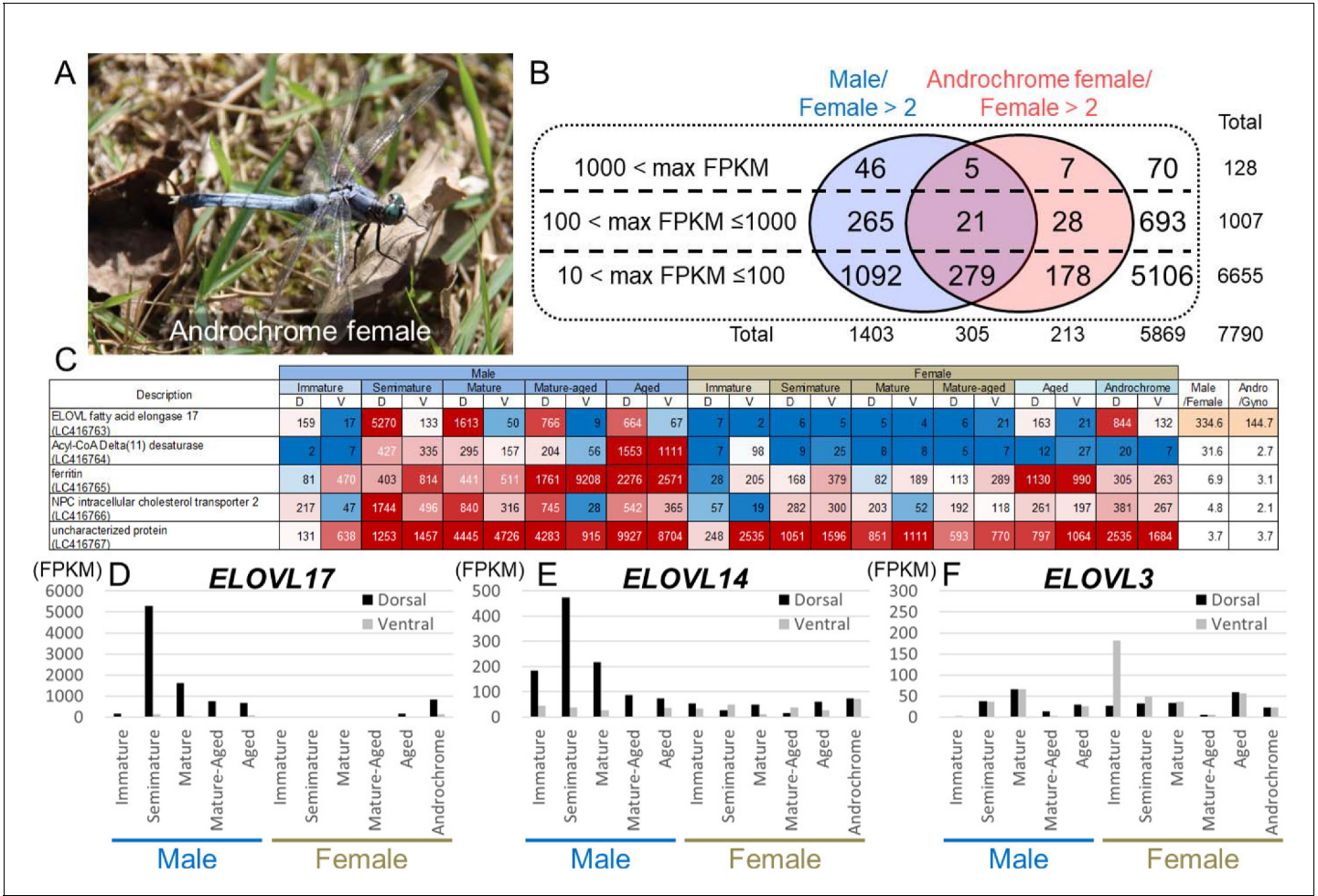


Figure 10. Genes associated with UV reflective wax. (A) An androchrome female used for transcriptome analysis. (B) The number of genes that were upregulated in the dorsal abdominal epidermis of males and/or an androchrome female compared to normal females. (C) The list of genes upregulated in the dorsal abdominal epidermis of both males and an androchrome female (max FPKM >1000). Gene expression levels are displayed as a heat map. The numbers indicate FPKM values. Red and blue fills indicate high and low expression levels, respectively. D and V indicate the dorsal and ventral parts of the epidermis of *O. albistylum*. (D–F) Expression level of three elongation of very long-chain fatty acids (ELOVL) genes in the dorsal and ventral parts of the epidermis of *O. albistylum*.

DOI: <https://doi.org/10.7554/eLife.43045.032>

| contig | Immature | | Semimature | | Mature | | Mature-aged | | Aged | | Immature | | Semimature | | Mature | | Mature-aged | | Aged | | Androchrome | | Description (Top hit) | E-value | Male /Female | Andro /Gyno | Max FPKM (Dorsal) |
|-------------------|----------|-----|------------|------|--------|------|-------------|------|------|------|----------|------|------------|------|--------|------|-------------|-----|------|------|-------------|-----------------------------------|--|-----------|--------------|-------------|-------------------|
| | D | V | D | V | D | V | D | V | D | V | D | V | D | V | D | V | D | V | D | V | D | V | | | | | |
| c153509R | 131 | 698 | 1253 | 1467 | 4445 | 4726 | 4283 | 915 | 9527 | 8704 | 248 | 2535 | 1051 | 1596 | 851 | 1111 | 693 | 770 | 797 | 1064 | 2535 | 1064 | NA | | 3.7 | 3.7 | 9927 |
| c147539R (ELOV17) | 159 | 17 | 5270 | 133 | 1013 | 50 | 706 | 9 | 904 | 67 | 7 | 2 | 5 | 5 | 5 | 4 | 5 | 21 | 163 | 21 | 844 | 132 | elongation of very long chain fatty acids protein AAEL008004 [Camponotus floridanus] | 3.00E-122 | 334.6 | 144.7 | 5270 |
| c148747R | 81 | 409 | 4938 | 814 | 545 | 511 | 1761 | 9208 | 2276 | 2571 | 28 | 205 | 163 | 379 | 82 | 189 | 113 | 289 | 1130 | 990 | 305 | 263 | NPC intracellular cholesterol transporter 2 [Agilus planipennis] | 1.00E-09 | 6.9 | 3.1 | 2276 |
| c153793R | 217 | 47 | 1744 | 490 | 840 | 316 | 745 | 28 | 542 | 385 | 57 | 19 | 282 | 300 | 203 | 52 | 192 | 118 | 261 | 197 | 381 | 287 | Acyl-CoA Delta(11) desaturase [Zootermopsis nevadensis] | 2.00E-44 | 4.8 | 2.1 | 1744 |
| c145398R | 2 | 7 | 727 | 335 | 295 | 157 | 204 | 55 | 1593 | 1111 | 7 | 98 | 9 | 25 | 8 | 8 | 5 | 7 | 12 | 27 | 20 | 7 | Serine protease inhibitor VIII-like has perleu | 0 | 31.6 | 2.7 | 1593 |
| c143830R | 15 | 8 | 110 | 12 | 655 | 19 | 89 | 5 | 47 | 93 | 15 | 12 | 12 | 4 | 9 | 7 | 8 | 18 | 57 | 18 | 55 | 38 | elongation of very long chain fatty acids protein AAEL008004 [Camponotus floridanus] | 4.00E-24 | 20.9 | 5.1 | 659 |
| c143423R | 185 | 44 | 473 | 37 | 217 | 26 | 87 | 3 | 73 | 36 | 54 | 33 | 27 | 49 | 49 | 11 | 16 | 38 | 60 | 27 | 73 | 73 | NA | | 6.6 | 2.0 | 473 |
| c145528R | 52 | 62 | 445 | 78 | 238 | 54 | 148 | 15 | 258 | 166 | 38 | 65 | 63 | 71 | 76 | 21 | 26 | 47 | 78 | 88 | 200 | 126 | mid-1-interacting protein 1-like [Zootermopsis nevadensis] | 3.00E-70 | 4.4 | 4.0 | 445 |
| c139526R | 1 | 0 | 91 | 144 | 33 | 54 | 97 | 47 | 54 | 211 | 1 | 1 | 11 | 1 | 45 | 27 | 15 | 4 | 370 | 0 | 37 | 59 | CG9269 [Drosophila melanogaster] | 5.00E-16 | 3.1 | 2.1 | 370 |
| c149278R | 18 | 9 | 284 | 139 | 174 | 64 | 98 | 4 | 111 | 70 | 12 | 16 | 33 | 26 | 52 | 10 | 9 | 11 | 31 | 18 | 53 | 21 | acetyl-coenzyme A synthetase [Zootermopsis nevadensis] | 0 | 5.9 | 2.0 | 284 |
| c149555R | 3 | 0 | 29 | 48 | 130 | 142 | 275 | 48 | 5 | 9 | 0 | 18 | 55 | 32 | 44 | 34 | 47 | 9 | 5 | 49 | 31 | CG34166 [Drosophila melanogaster] | 1.00E-10 | 5.3 | 2.4 | 275 | |
| c153289R | 262 | 805 | 93 | 133 | 143 | 187 | 167 | 29 | 79 | 99 | 28 | 92 | 84 | 124 | 97 | 78 | 57 | 71 | 296 | 278 | 227 | 89 | apolipoprotein D-like [Zootermopsis nevadensis] | 4.00E-66 | 2.5 | 3.4 | 262 |
| c151984R | 1 | 3 | 32 | 33 | 114 | 51 | 31 | 4 | 248 | 179 | 1 | 2 | 6 | 5 | 11 | 14 | 5 | 5 | 8 | 9 | 41 | 14 | trehalose-6-phosphate synthase 1 [Blattella germanica] | 0 | 8.0 | 7.3 | 248 |
| c149439R | 0 | 0 | 205 | 20 | 0 | 0 | 24 | 1 | 4 | 17 | 11 | 1 | 1 | 0 | 0 | 7 | 6 | 20 | 0 | 0 | 22 | 42 | tyrosine 3-monooxygenase [Zootermopsis nevadensis] | 0 | 13.2 | 5.0 | 205 |
| c149196R | 33 | 27 | 48 | 51 | 109 | 114 | 142 | 107 | 108 | 90 | 27 | 51 | 1 | 8 | 23 | 15 | 72 | 101 | 60 | 51 | 197 | 213 | 40S ribosomal protein S15 [Blattella germanica] | 2.00E-64 | 2.7 | 6.4 | 197 |
| c150068R | 3 | 14 | 55 | 76 | 51 | 37 | 192 | 43 | 142 | 97 | 5 | 38 | 21 | 34 | 14 | 14 | 8 | 10 | 27 | 37 | 25 | 11 | mitochondrial basic amino acids transporter [Cryptotermes secundus] | 8.00E-104 | 6.1 | 2.1 | 192 |
| c146712R | 71 | 30 | 157 | 166 | 20 | 15 | 70 | 65 | 14 | 0 | 2 | 1 | 8 | 6 | 12 | 3 | 3 | 8 | 31 | 33 | 14 | 49 | cystathionine gamma-lyase [Crassostrea gigas] | 0 | 13.1 | 2.3 | 167 |
| c148028R | 23 | 4 | 155 | 8 | 40 | 5 | 20 | 1 | 14 | 4 | 6 | 4 | 9 | 7 | 3 | 2 | 2 | 5 | 5 | 2 | 18 | 13 | putative fatty acyl-CoA reductase [Cryptotermes secundus] | 0 | 12.3 | 3.7 | 155 |
| c154118R | 10 | 5 | 48 | 98 | 141 | 122 | 55 | 15 | 105 | 88 | 3 | 8 | 4 | 0 | 49 | 62 | 16 | 29 | 38 | 52 | 51 | 39 | caraspilin-like [Crassus abietinus] | 2.00E-18 | 3.5 | 3.3 | 141 |
| c153348R | 41 | 87 | 130 | 63 | 34 | 45 | 23 | 32 | 88 | 73 | 21 | 19 | 42 | 35 | 30 | 22 | 20 | 26 | 48 | 40 | 60 | 19 | ATP-binding cassette sub-family G member 4 [Cryptotermes secundus] | 0 | 2.0 | 2.1 | 130 |
| c149130R | 40 | 11 | 125 | 39 | 37 | 31 | 20 | 3 | 28 | 13 | 13 | 5 | 9 | 7 | 25 | 2 | 10 | 13 | 46 | 17 | 32 | 41 | Serine protease inhibitor 88Ea [Blattella germanica] | 5.00E-95 | 3.9 | 2.2 | 125 |
| c150904R | 60 | 262 | 63 | 68 | 120 | 125 | 101 | 25 | 80 | 78 | 16 | 75 | 61 | 95 | 46 | 51 | 40 | 48 | 93 | 96 | 91 | 29 | hypothetical protein B7P43_G14218 [Cryptotermes secundus] | 3.00E-58 | 2.1 | 2.2 | 120 |
| c147603R | 38 | 137 | 71 | 85 | 119 | 135 | 68 | 32 | 38 | 35 | 2 | 41 | 3 | 4 | 0 | 0 | 38 | 63 | 11 | 21 | 34 | 20 | Regenectin [Periplaneta americana] | 4.00E-51 | 6.7 | 3.1 | 119 |
| c153322R | 0 | 0 | 92 | 69 | 13 | 32 | 119 | 63 | 11 | 17 | 0 | 4 | 14 | 28 | 2 | 8 | 2 | 11 | 13 | 29 | 39 | 14 | tyrosine/alpha-aminoacidate aminotransferase [Habropoda laboriosa] | 2.00E-130 | 12.4 | 8.7 | 119 |
| c148957R | 1 | 6 | 49 | 55 | 72 | 48 | 95 | 19 | 118 | 88 | 0 | 7 | 4 | 3 | 23 | 32 | 13 | 17 | 21 | 19 | 29 | 13 | NA | | 5.4 | 2.9 | 118 |
| c148343R | 1 | 6 | 27 | 35 | 54 | 45 | 41 | 10 | 117 | 60 | 1 | 7 | 5 | 3 | 2 | 2 | 4 | 2 | 35 | 52 | 28 | 14 | chitinotriase-1 [Mesochorus rotundata] | 8.00E-26 | 10.1 | 9.2 | 117 |
| c149270R | 9 | 5 | 54 | 29 | 102 | 88 | 35 | 15 | 40 | 32 | 23 | 19 | 40 | 30 | 29 | 13 | 8 | 20 | 7 | 2 | 54 | 45 | pyruvate kinase-like 5 [Cryptotermes secundus] | 0 | 2.1 | 2.2 | 102 |

Figure 10—figure supplement 1. List of genes that are upregulated in the dorsal abdominal epidermis of both males and an androchrome female (max FPKM >100). Gene expression levels are displayed as a heat map. The numbers indicate FPKM values. Red and blue fills indicate high and low expression levels, respectively. D and V indicate the dorsal and ventral abdominal regions, respectively. Andro and Gyno mean androchrome and normal (gynochrome) females, respectively.

DOI: <https://doi.org/10.7554/eLife.43045.033>

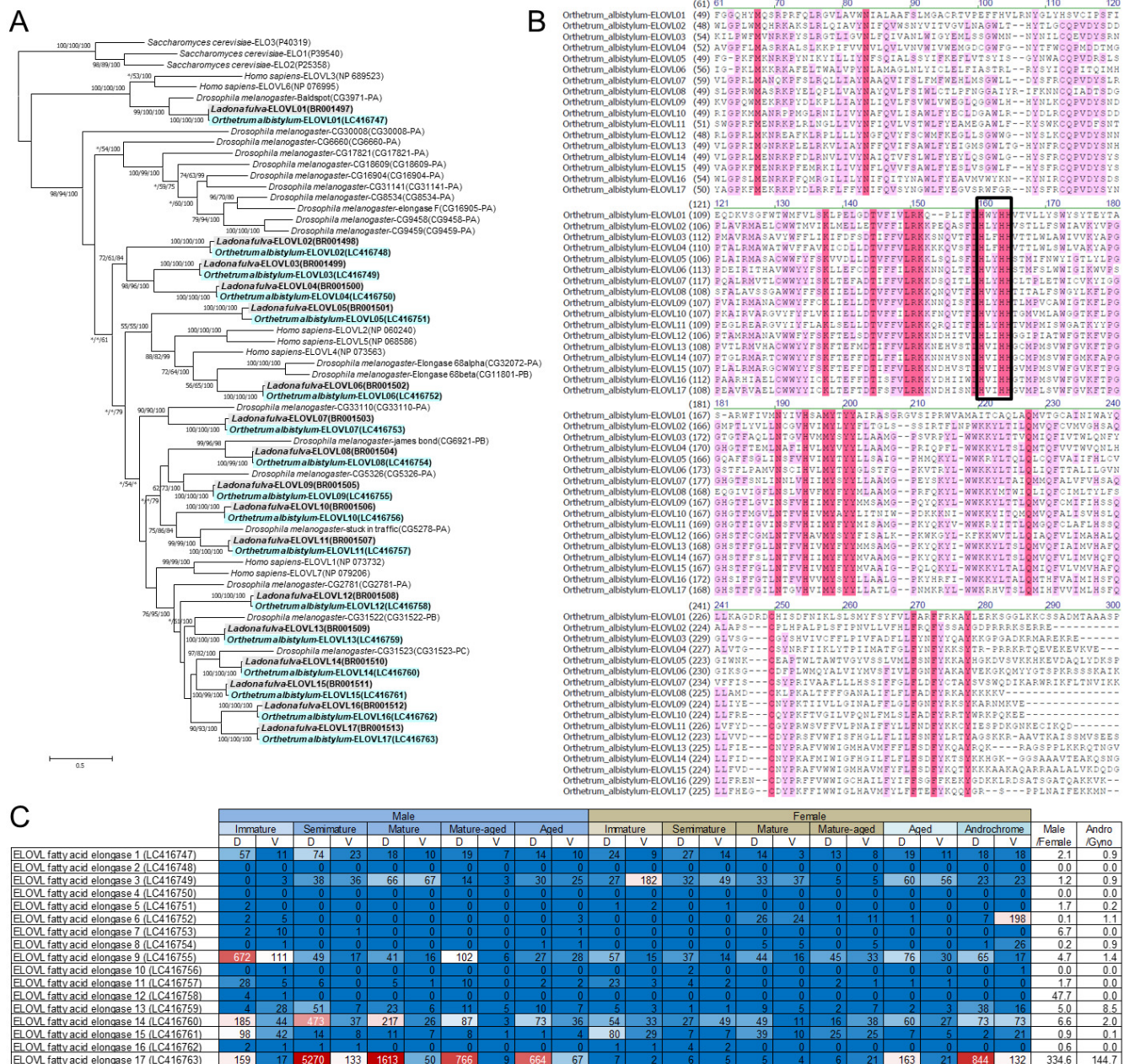


Figure 11. Identification of 17 ELOVL genes in dragonflies. (A) Phylogenetic tree of ELOVL family genes produced on the basis of their amino-acid sequences. A maximum likelihood phylogeny is shown, but neighbor-joining and Bayesian phylogenies exhibit substantially the same topologies. Statistical supporting values are indicated for each node (shown as (bootstrap value of neighbor-joining)/(bootstrap value of maximum likelihood)/(posterior probability of Bayesian)). Asterisks indicate support values < 50%. Blue and gray shading indicates *O. albistylum* and *L. fulva* genes, respectively. Accession numbers or annotation identities are shown in parentheses. (B) Alignment of 17 ELOVL genes of *O. albistylum*. The conserved histidine motif is boxed. (C) Gene expression levels of 17 ELOVL genes in *O. albistylum*. The numbers indicate FPKM values. Red and blue shading indicates high and low expression levels, respectively. D and V indicate the dorsal and ventral abdominal regions, respectively.

DOI: <https://doi.org/10.7554/eLife.43045.034>